

Synthesis and Evaluation of Mycophenolic Acid Derivatives as Potential Anti-*Toxoplasma Gondii* Agents

Fan-Fan Shang

Yanbian University

Mei-Yuan Wang

Yanbian University

Jiang-Ping Ai

Yanbian University

Qing-Kun Shen

Yanbian University

Hong-Yan Guo

Yanbian University

Chun-Mei Jin

Yanbian University

Fen-Er Chen

Fudan University

Zhe-Shan Quan

Yanbian University

Lili Jin

Yanbian University

Changhao Zhang (✉ zhangch@ybu.edu.cn)

Yanbian University

Research Article

Keywords: Mycophenolic acid, Synthesis, *Toxoplasma gondii*, in vitro, in vivo

Posted Date: August 10th, 2021

DOI: <https://doi.org/10.21203/rs.3.rs-780085/v1>

License:   This work is licensed under a Creative Commons Attribution 4.0 International License.

[Read Full License](#)

Abstract

Nineteen mycophenolic acid (MPA) derivatives were designed and synthesized, and their anti-*Toxoplasma* activity evaluated for the first time. Among them, *N*-propylimidazole-modified compound **E5** demonstrated the strongest activity, and the IC₅₀ against HFF-1 (Human Foreskin Fibroblasts-1) cells following infection with *T. gondii* is 80.9 μM (MPA-211.5 μM) and its selectivity value is 2.2 (MPA-1.2). *In vivo* experiments, **E5** significantly inhibited the proliferation of tachyzoites in the abdominal cavity of mice acutely infected with *T. gondii* (inhibition rates 46.7%), and this inhibitory effect was greater than that of spiramycin (inhibition rates 31.3%) and MPA (inhibition rates 15.9%), this indicated that **E5** had significant protective effects on the host during acute *Toxoplasma* infection. In addition **E5** significantly reduced the levels of alanine aminotransferase (ALT) and aspartate aminotransferase (AST) in the serum of infected mice, significantly increased the level of glutathione (GSH) in the liver, and significantly reduced the level of malondialdehyde (MDA), indicating that it has a significant hepatoprotective effect against *T. gondii* infection. Similarly, **E5** can relieve hepatomegaly and splenomegaly induced by acute *Toxoplasma* infection. Spiramycin aggravated appetite loss in infected mice, while **E5** did not. In summary, the results indicated that **E5** has potential as a candidate anti-*T. gondii* drug.

1. Introduction

Toxoplasma gondii is an obligate intracellular parasite with a wide variety of hosts, including humans, livestock, and marine mammals, and can cause zoonotic toxoplasmosis^[1]. Following infection, individuals with normal immune function show no obvious symptoms, while those with insufficient or low immune function may display extensive pathological damage or even death. In pregnant females, infection can lead to miscarriage, premature delivery, stillbirth, and teratogenesis^[2, 3]. *Toxoplasma gondii* can also infect domestic animals, such as pigs, cattle, and sheep, and often infects companion animals, such as dogs, cats, and rabbits. The pathogen also causes huge economic losses to the livestock industry, and *T. gondii* is detrimental to food safety and human health^[4, 5]. At present, the main treatment for toxoplasmosis is still drug therapy, mainly including pyrimethamine, sulfadiazine, spiramycin and the combined use of sulfadiazine and pyrimethamine. Although there has been some success with anti-*Toxoplasma* drugs, many problems remain. For example, the use of anti-*Toxoplasma* drugs can lead to adverse reactions, such as allergies, bone marrow suppression, and increased risk of liver and kidney complications. In addition, these drugs are not suitable for use during pregnancy^[6–8]. Therefore, there is an urgent need for the development of anti-*Toxoplasma* drugs with high efficiency and low toxicity.

The immunosuppressant mycophenolate mofetil has been used widely to prevent and treat the acute rejection of transplanted organs. Mycophenolate mofetil exerts immunosuppressive activity via conversion into mycophenolic acid (MPA, Fig. 1) in the body^[9–11]. MPA is a meroterpenoid consisting of an acetate-derived phthalide nucleus and a terpene-derived side chain, which possesses a range of biological properties, including antifungal^[12], antiviral^[13], anti-inflammatory^[14], and antitumor^[15] properties. In addition, MPA is a potent non-competitive inhibitor of inosine nucleotide dehydrogenase

inosine monophosphate dehydrogenase (IMPDH). However, IMPDH is essential for the purine metabolism of *Toxoplasma gondii*. More importantly, MPA has been used extensively in strategies for the generation of genetically modified strains of *Toxoplasma gondii*^[16]. To our knowledge, there have been no reports on the activity of MPA derivatives against *T. gondii*. Therefore, in this study, we modified the structure of MPA to obtain high-efficiency and low-toxicity anti-*Toxoplasma* drugs.

Studies have reported that the lactone ring and aromatic methyl group in the structure of MPA are essential to its activity^[17]. Therefore, in this study, these two groups were retained, and the carboxyl position of the structure was modified to introduce nitrogen-containing pharmacophores and convert it into an amide. The amide group can be used as a hydrogen donor, reducing the sensitivity of enzymatic hydrolysis and improving the stability of the compound in vivo and in vitro^[18]. Amino acids are the basic biological and functional units of proteins; and they play a vital role in human metabolism and exert a wide range of biological activities, including antibacterial^[19, 20], anticancer^[21], anti-tuberculosis^[22], anti-inflammatory^[23, 24], and anti-parasitic^[25, 26] activities. In addition, they improve both the solubility and bioavailability of the drugs^[27–29]. Studies have reported that nitrogen-containing heterocycles, such as benzylamine, pyrrolidine, piperazine, morpholine, and imidazole, are an important class of active fragments against *T. gondii*^[30–32]. In addition, active fragments with these functions also include benzylamine and fatty amines^[29]. Therefore, we designed and synthesized five series of MPA derivatives and evaluated their anti-*Toxoplasma* activity. Subsequently, we selected the most active derivative **E5**, at the cellular level for subsequent in vivo activity studies to find highly efficient and low-toxicity MPA derivatives with anti-*Toxoplasma* activity.

2. Results And Discussion

2.1 Chemistry

The synthetic route for targets is shown in **Scheme 1**. MPA as a starting material and all target compounds were obtained by an amide condensation reaction with different amino compounds catalysed by 1-(3-dimethylaminopropyl)-3-ethylcarbodiimide hydrochloride (EDCI) and Biphenyl-4-amidoxime (HOBT) in anhydrous CH₂Cl₂ at 0°C^[33,34]. TLC was used to monitor the reactions, and the final products were purified using silica gel chromatography to obtain the target compounds. Among them, compounds **A1**, **A3**, **A4**, **C1**, **C2**, **E3** have been reported^[35,36]. All compounds were confirmed by ¹H NMR, ¹³C NMR, and high-resolution mass spectrometry.

2.2 Biological evaluation

2.2.1 In vitro anti-*T. gondii* activity and Structure-activity relationship (SAR) study

The thiazolyl blue (MTT) colorimetric method was used to determine the cytotoxicity and in vitro anti-tachyzoites activity (*T. gondii*, RH strain) of all compounds at different concentrations (10 – 1000 µM) in an activity test in host cells (Human Foreskin Fibroblasts-1 cells)^[37].

The *in vitro* anti-*Toxoplasma* activity is shown in **Table 1**. IC_{50}^a is the half-inhibitory concentration of the compound against HFF-1 cells, which reflects its cytotoxicity. IC_{50}^b is the half-inhibitory concentration of the compound against HFF-1 cells following infection with *T. gondii*; this value reflects the anti-*T. gondii* activity of the compound. The selectivity index (SI = IC_{50}^a/IC_{50}^b) provides a screening reference for subsequent *in vivo* experiments^[18]. In this experiment, MPA was used as the lead compound, different types of pharmacophores were introduced, and five series of compounds were designed and synthesised with spiramycin being used as the positive control drug. The anti-*Toxoplasma* activity of MPA *in vitro* was greater than that of spiramycin, which has strong anti-*Toxoplasma* potential. In the compound **A** series, different substituted aromatic hydrocarbons were introduced into the MPA. The *in vitro* anti-*Toxoplasma* activity of all compounds was lower than that of lead, however it is worth noting that most of the compounds showed very low cytotoxicity, except for **A1**, the selectivity of all compounds has been improved, and their SI value was higher than that of MPA and the positive control drugs. In this series, the preliminary structure-activity relationship demonstrated that the introduction of electron-withdrawing groups or electron-donating groups on the benzene ring, or appropriately extended the length of the aliphatic chain, increased the *in vitro* anti-*Toxoplasma* activity. In the compound **B** series, different alkanes were introduced into the MPA. Compared with that of the lead, all compounds demonstrated reduced *in vitro* anti-*Toxoplasma* activity and a lower SI value. This suggests that the introduction of alkanes on MPA decreased the effectiveness against *T. gondii*. The compound **C** series was endowed with different amino acid methyl ester fragments into the lead. In this group, compound **C1** and lead exhibited similar *in vitro* anti-*Toxoplasma* activity. The SI value of compound **C2** was 1.6, which was better than that of the lead and the positive control drugs. In the compound **D** series, four different amine compounds were connected to MPA. Unfortunately, the *in vitro* anti-*Toxoplasma* activity and SI values of all compounds were not ideal. The compound **E** series are connected to different heterocyclic compounds, and the *in vitro* anti-*Toxoplasma* activity of compounds **E3**, **E4**, and **E5** were improved. Compound **E5** obtained by the introduction of an *N*-propylimidazole fragment to the lead, and this compound presented the strongest *in vitro* anti-*Toxoplasma* activity among all series, and the IC_{50} against HFF-1 cells following infection with *T. gondii* is 80.9 μ M. In addition, it has the highest selectivity in this article (SI: 2.2), its IC_{50} and SI values were significantly better than those of the positive control drug (IC_{50} : 233.4 μ M; SI:1.2) and mycophenolic acid (IC_{50} : 211.5 μ M; SI:1.2), which indicates that it has the highest selectivity index while maintaining *in vitro* anti-*Toxoplasma* activity and has some research value. Therefore, in this experiment, compound **E5** was selected for the subsequent evaluation of anti-*T. gondii* activity *in vivo*.

2.2.2 Effect of compounds **E5** on the inhibition of tachyzoites *in vivo*

The number of *T. gondii* tachyzoites in the abdominal cavity of mice reflects the therapeutic effects of a compound^[38]. As shown in **Table 2** and **Figure 2**, compared with that of the model group, after treatment with 100 mg/kg of different compounds,

the inhibition of intraperitoneal tachyzoites in mice in the MPA treatment group was only 15.9%. Interestingly, intraperitoneal tachyzoite inhibition in the **E5** treatment groups was 46.7%, respectively, and there were significant differences compared with the model group ($p < 0.001$). Therefore, compound **E5** significantly reduced the number of *T. gondii* tachyzoites in the abdominal cavity of Kunming mice and their activity exceeded that of the positive control spiramycin, indicating that **E5** is effective against acute *T. gondii* infection. The protective effect on the host during infection was significant.

2.2.3 Liver and spleen indices.

A large number of studies have shown that in the acute infection model obtained by giving a virulent strain of *Toxoplasma gondii* through the abdominal cavity of mice, it is found that the liver is an important place for toxoplasma replication. *Toxoplasma gondii* is produced in large quantities in liver cells, which damages the liver cells^[39], leading to liver pathological changes such as hepatomegaly, hepatitis, and necrosis in the infected host. Hepatic function and metabolism reduce when hepatocytes are damaged. Therefore incomplete metabolized substances are produced in liver, resulting in an increase on the liver index^[40]. The level of the liver index reflects the degree of liver damage^[41]. Moreover, the spleen is an important immune organ, which plays a significant role in the immune response, including the response to antigenic substances in the blood. Both humoral and cellular immunity can induce changes in the organizational structure of the spleen. To a certain extent, an increase in the spleen index reflects changes in spleen structure and function^[42,43]. Therefore, the liver and spleen indices can be used to evaluate the protective effects of drugs on organs. As shown in **Figure 3**, compared with those in the normal group, the liver and spleen indices of the toxo group increased, indicating that *T. gondii* induces liver and spleen damage in mice. Compound **E5** was able to alleviate hepatomegaly and splenomegaly caused by acute *Toxoplasma* infection.

2.2.4 ALT and AST in serum

The levels of alanine aminotransferase (ALT) and aspartate aminotransferase (AST) in serum are used to evaluate liver function. In this experiment, the liver toxicity of each compound was evaluated by determining the levels of ALT and AST in the serum of mice^[44]. As shown in **Figure 4**, compared with those in the normal group, the ALT and AST levels in the toxo group were significantly increased, and this was alleviated in the treatment group. Notably, compound **E5** was able to significantly reduce the levels of ALT and AST in the serum of infected mice. These results show that compound **E5** is effective in treating *T. gondii* infection and preventing hepatotoxicity caused by *T. gondii* infection.

2.2.5 GSH and MDA

Glutathione (GSH) is a small-molecule peptide composed of three amino acids that is involved in detoxification, its main functions are to scavenge free radicals, resist oxidation, and resist aging^[45]. According to reports in the literature, *Toxoplasma gondii* infection can cause oxidative stress and immunosuppressive reactions^[46]. During the infection of *Toxoplasma gondii*, the production of reactive

oxygen species ROS increases, and the excessive production of ROS can cause cell and tissue damage^[47,48]. GSH can protect cells from oxidative damage by eliminating superoxide anion free radicals. And its levels in mice exposed to *Toxoplasma gondii* are significantly reduced^[49,50]. As shown in **Figure 5 A**, compared with the normal group, the GSH content of the toxo group was significantly reduced, indicating that *T. gondii* infection can decrease the GSH content in mice. Interestingly, compared with that of the model group, GSH content was increased in mice in the treatment group, and the activity of compound **E5** was greater than that of the positive control spiramycin and the lead compound MPA. This indicates that compound **E5** is effective at inhibiting the growth of *T. gondii* in mice and has a strong antioxidant effect.

Malondialdehyde (MDA), one major product of lipid peroxidation, significantly increased in mice exposed to *T. gondii*^[51]. As shown in **Figure 5 B**, compared with that of the normal group, the MDA content in the toxo group significantly increased as we predicted, while spiramycin, MPA and **E5** significantly reduced MDA content. Among them, compound **E5** had the same curative effect as spiramycin and was better than lead MPA.

2.2.6 Effects of compounds on the weight of mice

To further evaluate the effects of the test compounds on mice, the weight change of animals during treatment was recorded. As shown in **Figure 6**, compared with the normal group, mice in the toxo group lost their appetite due to *T. gondii* infection, resulting in a sharp decline in body weight. However, this was exacerbated by spiramycin and MPA. Notably, compound **E5** did not result in weight loss, moreover alleviated the loss of appetite in mice.

3. Conclusions

In this study, nineteen MPA derivatives in five series were designed and synthesised, and their anti-*Toxoplasma* activity was reported for the first time. The *in vitro* results demonstrated that **E5** was the greatest potential and was superior to MPA and spiramycin.. The results of further *in vivo* experiments showed that **E5** exerted an inhibitory effect on *T. gondii*, a strong protective effect on the liver, and could significantly alleviate splenomegaly in infected mice with limited side effects. These findings suggest that **E5** is a potential candidate anti-*T. gondii*. drug.

4. Experimental Section

Mycophenolic acid is a natural compound, purchased from Chengdu Refines Biotechnology Co., Ltd., with a purity of 98%. The organic reagents required for the experiment are all analytically pure, and other chemicals are purchased from Aladdin reagent. The obtained products were monitored by thin-layer chromatography to check the progress of the reaction, and separation was carried out using a chromatography column. The melting point of the target product was measured in an open capillary (the temperature is not corrected); ¹H-NMR and ¹³C-NMR used the chemical shift of TMS as the zero point,

measured by AV-300 nuclear magnetic resonance instrument; The high resolution mass spectrum was measured by ESI mass spectrometer.

4.1 General procedure for the reaction of mycophenolic acid with different intermediates containing-amino

Mycophenolic acid (64 mg, 0.2 mmol), different amine compounds (0.24 mmol), carboxylic mixture 1-Ethyl-3-(3-dimethylaminopropyl) carbodiimide hydrochloride (EDCI) (114.7 mg, 0.6 mmol) and catalyst Biphenyl-4-amidoxime (HOBt) (84.8 mg, 0.4 mmol) were taken in a 25 ml round bottom flask, and 5 ml dichloromethane as solvent, stirred at 0 °C for 4-6 h, progress of reaction was confirmed by TLC, the final products were purified using silica gel chromatography, and all the target compounds were obtained, which are white powder in appearance, and the yield is 48%-79%.

4.1.1 (E)-N-benzyl-6-(4-hydroxy-6-methoxy-7-methyl-3-oxo-1,3-dihydroisobenzofuran-5-yl)-4-methylhex-4-enamide (A1)

White powder; yield 52%; m.p. 96-98°C. ¹H NMR (300 MHz, CDCl₃, ppm) δ 7.67 (s, 1H), 7.35-7.30 (m, 2H), 7.27-7.20 (m, 3H), 5.77 (brs, 1H), 5.32 (t, *J* = 8.1 Hz, 1H), 5.19 (s, 2H), 4.41 (d, *J* = 5.7 Hz, 2H), 3.77 (s, 3H), 3.40 (d, *J* = 6.9 Hz, 2H), 2.36 (s, 4H), 2.15 (s, 3H), 1.84 (s, 3H). ¹³C NMR (75 MHz, CDCl₃): δ 172.91, 172.48, 163.63, 153.59, 144.04, 138.33, 134.60, 128.62 (2C), 127.58 (2C), 127.36, 123.06, 122.00, 116.76, 106.40, 70.03, 61.01, 43.48, 35.27, 35.09, 22.62, 16.12, 11.54. ESI-HRMS (*m/z*) calcd for C₂₄H₂₈NO₅⁺ [M+H]⁺: 410.19620, found: 410.19528.

4.1.2 (E)-N-(4-fluorobenzyl)-6-(4-hydroxy-6-methoxy-7-methyl-3-oxo-1,3-dihydroisobenzofuran-5-yl)-4-methylhex-4-enamide (A2)

White powder; yield 73%; m.p. 156-158°C. ¹H NMR (300 MHz, CDCl₃, ppm) δ 7.67 (s, 1H), 7.19 (dd, *J* = 8.4, 5.4 Hz, 2H), 6.98 (t, *J* = 8.7 Hz, 2H), 5.81 (brs, 1H), 5.29 (t, *J* = 6.9 Hz, 1H), 5.20 (s, 2H), 4.37 (d, *J* = 5.7 Hz, 2H), 3.77 (s, 3H), 3.40 (d, *J* = 6.9 Hz, 2H), 2.36 (s, 4H), 2.15 (s, 3H), 1.83 (s, 3H). ¹³C NMR (75 MHz, CDCl₃): δ 172.90, 172.55, 163.68, 163.61, 153.58, 144.05, 134.57, 134.23, 129.24, 129.14, 123.10, 121.94, 116.80, 115.52, 115.24, 106.39, 70.05, 61.01, 42.70, 35.24, 34.99, 22.64, 16.10, 11.53. ESI-HRMS (*m/z*) calcd for C₂₄H₂₇FNO₅⁺ [M+H]⁺: 428.18678, found: 428.18616.

4.1.3 (E)-6-(4-hydroxy-6-methoxy-7-methyl-3-oxo-1,3-dihydroisobenzofuran-5-yl)-4-methyl-N-(4-methylbenzyl)hex-4-enamide (A3)

White powder; yield 75%; m.p. 116-118°C. ¹H NMR (300 MHz, CDCl₃, ppm) δ 7.68 (s, 1H), 7.12 (s, 4H), 5.75 (brs, 1H), 5.28 (t, *J* = 6.6 Hz, 1H), 5.19 (s, 2H), 4.35 (d, *J* = 5.7 Hz, 2H), 3.77 (s, 3H), 3.40 (d, *J* = 6.6 Hz, 2H), 2.34 (s, 7H), 2.15 (s, 3H), 1.82 (s, 3H). ¹³C NMR (75 MHz, CDCl₃): δ 172.90, 172.41, 163.64, 153.60, 144.03, 137.07, 135.29, 134.61, 129.28 (2C), 127.60 (2C), 122.99, 122.03, 116.75, 106.39, 70.03, 61.00,

43.25, 35.29, 35.14, 22.62, 21.07, 16.12, 11.55. ESI-HRMS (m/z) calcd for $C_{25}H_{30}NO_5^+$

$[M+H]^+$: 424.21185, found: 424.2115.

4.1.4 (E)-6-(4-hydroxy-6-methoxy-7-methyl-3-oxo-1,3-dihydroisobenzofuran-5-yl)-4-methyl-N-phenethylhex-4-enamide (A4)

White powder; yield 70%; m.p. 102-104°C. 1H NMR (300 MHz, $CDCl_3$, ppm) δ 7.69 (brs, 1H), 7.34-7.29 (m, 2H), 7.25 (d, $J = 7.2$ Hz, 1H), 7.21-7.12 (m, 2H), 5.49 (brs, 1H), 5.25 (t, $J = 6.9$ Hz, 1H), 5.13 (s, 2H), 3.78 (s, 3H), 3.48-3.38 (m, 4H), 2.70 (t, $J = 6.9$ Hz, 2H), 2.35-2.22 (m, 4H), 2.14 (s, 3H), 1.81 (s, 3H). ^{13}C NMR (75 MHz, $CDCl_3$) δ 172.92, 172.55, 163.66, 153.59, 144.09, 138.92, 134.57, 128.67 (2C), 128.59 (2C), 126.46, 122.81, 122.05, 116.77, 106.38, 70.02, 61.01, 40.53, 35.66, 35.22, 35.05, 22.61, 16.13, 11.55. ESI-HRMS (m/z) calcd for $C_{25}H_{30}NO_5^+$ $[M+H]^+$: 424.21185, found: 424.2115.

4.1.5 (E)-6-(4-hydroxy-6-methoxy-7-methyl-3-oxo-1,3-dihydroisobenzofuran-5-yl)-N-(4-hydroxyphenethyl)-4-methylhex-4-enamide (A5)

White powder; yield 70%; m.p. 112-114°C. 1H NMR (300 MHz, $CDCl_3$, ppm) δ 7.60 (brs, 2H), 6.92 (d, $J = 8.4$ Hz, 2H), 6.77 (d, $J = 7.2$ Hz, 2H), 5.85 (t, $J = 5.7$ Hz, 1H), 5.24 (t, $J = 6.9$ Hz, 1H), 5.09 (s, 2H), 3.76 (s, 3H), 3.40-3.34 (m, 4H), 2.56 (t, $J = 7.2$ Hz, 2H), 2.28 (s, 4H), 2.11 (s, 3H), 1.79 (s, 3H). ^{13}C NMR (75 MHz, $CDCl_3$): δ 173.35, 173.07, 163.67, 155.19, 153.53, 144.20, 134.36, 129.83, 129.58(2C), 123.01, 122.03, 116.85, 115.57(2C), 106.33, 70.12, 61.03, 40.95, 35.22, 34.94, 34.65, 22.62, 16.06, 11.54. ESI-HRMS (m/z) calcd for $C_{25}H_{30}NO_6^+$ $[M+H]^+$: 440.20676, found: 440.20621.

4.1.6 (E)-N-butyl-6-(4-hydroxy-6-methoxy-7-methyl-3-oxo-1,3-dihydroisobenzofuran-5-yl)-4-methylhex-4-enamide (B1)

White powder; yield 58%; m.p. 76-78°C. 1H NMR (300 MHz, $CDCl_3$, ppm) δ 7.70 (s, 1H), 5.46 (brs, 1H), 5.28 (t, $J = 7.2$ Hz, 1H), 5.22 (s, 2H), 3.79 (s, 3H), 3.41 (d, $J = 6.9$ Hz, 2H), 3.20 (dd, $J = 12.6, 6.0$ Hz, 2H), 2.35-2.23 (m, 4H), 2.17 (s, 3H), 1.83 (s, 3H), 1.47-1.25 (m, 4H), 0.91 (t, $J = 7.2$ Hz, 3H). ^{13}C NMR (75 MHz, $CDCl_3$): δ 172.93, 172.56, 163.69, 153.62, 144.03, 134.72, 122.80, 122.10, 116.79, 106.37, 70.07, 61.02, 39.18, 35.33, 35.18, 31.68, 22.62, 20.04, 16.13, 13.72, 11.57. ESI-HRMS (m/z) calcd for $C_{21}H_{30}NO_5^+$ $[M+H]^+$: 376.21185, found: 376.21127.

4.1.7 (E)-6-(4-hydroxy-6-methoxy-7-methyl-3-oxo-1,3-dihydroisobenzofuran-5-yl)-4-methyl-N-pentylhex-4-enamide (B2)

White powder; yield 65%; m.p. 108-110°C. 1H NMR (300 MHz, $CDCl_3$, ppm) δ 7.70 (s, 1H), 5.47 (brs, 1H), 5.27 (t, $J = 6.9$ Hz, 1H), 5.22 (s, 2H), 3.78 (s, 3H), 3.41 (d, $J = 6.9$ Hz, 2H), 3.22-3.15 (m, 2H), 2.36-2.26 (m, 4H), 2.17 (s, 3H), 1.83 (s, 3H), 1.48-1.39 (m, 2H), 1.35-1.24 (m, 4H), 0.90 (t, $J = 6.6$ Hz, 3H). ^{13}C NMR (75 MHz, $CDCl_3$): δ 172.93, 172.51, 163.68, 153.63, 144.02, 134.74, 122.79, 122.10, 116.79, 106.38, 70.06,

61.02, 39.45, 35.33, 35.21, 29.31, 29.05, 22.62, 22.33, 16.14, 13.97, 11.57. ESI-HRMS (m/z) calcd for $C_{22}H_{32}NO_5^+$ $[M+H]^+$: 390.22750, found: 390.22690.

4.1.8 *(E)-N-hexyl-6-(4-hydroxy-6-methoxy-7-methyl-3-oxo-1,3-dihydroisobenzofuran-5-yl)-4-methylhex-4-enamide (B3)*

White powder; yield 63%; m.p. 106-108°C. 1H NMR (300 MHz, $CDCl_3$, ppm) δ 7.70 (s, 1H), 5.47 (brs, 1H), 5.27 (t, $J = 6.9$ Hz, 1H), 5.22 (s, 2H), 3.79 (s, 3H), 3.41 (d, $J = 6.9$ Hz, 2H), 3.22-3.15 (m, 2H), 2.35-2.24 (m, 4H), 2.17 (s, 3H), 1.83 (s, 3H), 1.47-1.37 (m, 2H), 1.28 (s, 6H), 0.90 (t, $J = 6.3$ Hz, 3H). ^{13}C NMR (75 MHz, $CDCl_3$): δ 172.92, 172.52, 163.68, 153.63, 144.02, 134.74, 122.80, 122.10, 116.78, 106.38, 70.06, 61.02, 39.49, 35.34, 35.21, 31.47, 29.59, 26.58, 22.62, 22.55, 16.14, 14.01, 11.57. ESI-HRMS (m/z) calcd for $C_{23}H_{34}NO_5^+$ $[M+H]^+$: 404.24315, found: 404.24274.

4.1.9

Methyl (E)-(6-(4-hydroxy-6-methoxy-7-methyl-3-oxo-1,3-dihydroisobenzofuran-5-yl)-4-methylhex-4-enoyl)glycinate (C1)

White powder; yield 70%; m.p. 98-100°C. 1H NMR (300 MHz, $CDCl_3$, ppm) δ 7.71 (brs, 1H), 6.01 (brs, 1H), 5.29 (t, $J = 6.9$ Hz, 1H), 5.22 (s, 2H), 3.99 (d, $J = 5.1$ Hz, 2H), 3.78 (s, 3H), 3.76 (s, 3H), 3.41 (d, $J = 6.9$ Hz, 2H), 2.35 (s, 4H), 2.16 (s, 3H), 1.83 (s, 3H). ^{13}C NMR (75 MHz, $CDCl_3$): δ 172.90, 172.82, 170.48, 163.66, 153.61, 144.05, 134.39, 123.08, 122.09, 116.77, 106.39, 70.05, 61.02, 52.34, 41.13, 35.05, 34.80, 22.62, 16.11, 11.56. ESI-HRMS (m/z) calcd for $C_{20}H_{26}NO_7^+$ $[M+H]^+$: 392.17038, found: 392.17004.

4.1.10

methyl (E)-(6-(4-hydroxy-6-methoxy-7-methyl-3-oxo-1,3-dihydroisobenzofuran-5-yl)-4-methylhex-4-enoyl)phenylalaninate (C2)

White powder; yield 67%; m.p. 82-84°C. 1H NMR (300 MHz, $CDCl_3$, ppm) δ 7.69 (s, 1H), 7.32-7.29 (m, 1H), 7.28-7.24 (m, 2H), 7.07 (dd, $J = 7.8$ Hz, 2.1 Hz, 2H), 5.92 (d, $J = 8.7$ Hz, 1H), 5.26 (t, $J = 6.9$ Hz, 1H), 5.17 (s, 2H), 4.90-4.83 (m, 1H), 3.78 (s, 3H), 3.72 (s, 3H), 3.40 (d, $J = 6.9$ Hz, 2H), 3.05 (t, $J = 5.4$ Hz, 2H), 2.30 (s, 4H), 2.15 (s, 3H), 1.81 (s, 3H). ^{13}C NMR (75 MHz, $CDCl_3$): δ 172.90, 172.09 (2C), 163.66, 153.60, 144.06, 135.90, 134.38, 129.20 (2C), 128.54 (2C), 127.09, 122.83, 122.05, 116.73, 106.38, 70.02, 61.01, 53.00, 52.28, 37.95, 35.00, 34.91, 22.61, 16.15, 11.57. ESI-HRMS (m/z) calcd for $C_{27}H_{32}NO_7^+$ $[M+H]^+$: 482.21733, found: 482.21692.

4.1.11 *(E)-N-(2-(dimethylamino)ethyl)-6-(4-hydroxy-6-methoxy-7-methyl-3-oxo-1,3-dihydroisobenzofuran-5-yl)-4-methylhex-4-enamide (D1)*

White powder; yield 79%; m.p. 76-78°C. ¹H NMR (300 MHz, CDCl₃, ppm) δ 7.44 (brs, 1H), 5.30-5.24 (m, 1H), 5.21 (s, 2H), 3.78 (s, 3H), 3.57 (dd, *J* = 10.2 Hz, 5.3 Hz, 2H), 3.40 (d, *J* = 6.7 Hz, 2H), 3.01 (t, *J* = 5.1 Hz, 2H), 2.72 (s, 6H), 2.36 (brs, 4H), 2.16 (s, 3H), 1.83 (s, 3H). ¹³C NMR (75 MHz, CDCl₃) δ 173.55, 172.82, 163.62, 153.82, 144.16, 134.66, 122.73, 122.32, 116.62, 106.44, 69.95, 61.05, 58.11, 44.05(2C), 35.13, 35.11, 34.98, 22.68, 16.24, 11.55. ESI-HRMS (*m/z*) calcd for C₂₁H₃₁N₂O₅⁺ [M+H]⁺: 391.22275, found: 391.22235.

4.1.12 (E)-N-(2-(diethylamino)ethyl)-6-(4-hydroxy-6-methoxy-7-methyl-3-oxo-1,3-dihydroisobenzofuran-5-yl)-4-methylhex-4-enamide (D2)

White powder; yield 73%; m.p. 60-62°C. ¹H NMR (300 MHz, CDCl₃) δ 6.76 (brs, 1H), 5.26 (t, *J* = 6.5 Hz, 1H), 5.21 (s, 2H), 3.78 (s, 3H), 3.40 (d, *J* = 6.9 Hz, 4H), 2.74 (d, *J* = 7.1 Hz, 6H), 2.32 (s, 4H), 2.16 (s, 3H), 1.83 (s, 3H), 1.13 (t, *J* = 7.1 Hz, 6H). ¹³C NMR (75 MHz, CDCl₃): δ 172.97, 172.78, 163.60, 154.61, 144.11, 134.53, 123.06, 122.37, 116.04, 106.41, 69.89, 61.01, 51.62, 46.75 (2C), 36.62, 35.28 (2C), 22.74, 16.21, 11.54, 11.18 (2C). ESI-HRMS (*m/z*) calcd for C₂₃H₃₅N₂O₅⁺ [M+H]⁺: 419.25405, found: 419.25369.

4.1.13 (E)-N-(2-(ethyl(isopropyl)amino)ethyl)-6-(4-hydroxy-6-methoxy-7-methyl-3-oxo-1,3-dihydroisobenzofuran-5-yl)-4-methylhex-4-enamide (D3)

White powder; yield 66%; m.p. 58-60°C. ¹H NMR (300 MHz, CDCl₃) δ 6.14 (brs, 1H), 5.25 (t, *J* = 5.8 Hz, 1H), 5.21 (s, 2H), 3.77 (s, 3H), 3.40 (d, *J* = 6.8 Hz, 2H), 3.21 (d, *J* = 5.3 Hz, 2H), 3.02 (t, *J* = 6.0 Hz, 2H), 2.57 (brs, 2H), 2.41 – 2.19 (m, 5H), 2.16 (s, 3H), 1.82 (s, 3H), 1.02 (d, *J* = 6.4 Hz, 12H). ¹³C NMR (75 MHz, CDCl₃): δ 172.94, 172.38, 163.69, 153.70, 144.01, 134.66, 122.50, 122.18, 116.68, 106.36, 70.04, 61.02 (2C), 47.68, 43.01, 37.90, 35.41, 35.37, 22.62, 20.78 (2C), 16.21 (2C), 11.57. ESI-HRMS (*m/z*) calcd for C₂₅H₃₉N₂O₅⁺ [M+H]⁺: 447.28535, found: 447.28503.

4.1.14 (E)-N-(2-acetamidoethyl)-6-(4-hydroxy-6-methoxy-7-methyl-3-oxo-1,3-dihydroisobenzofuran-5-yl)-4-methylhex-4-enamide (D4)

White powder; yield 72%; m.p. 98-100°C. ¹H NMR (300 MHz, CDCl₃) δ 7.71 (s, 1H), 6.26 (d, *J* = 23.9 Hz, 2H), 5.27 (dd, *J* = 15.0, 8.2 Hz, 1H), 5.22 (s, 2H), 3.78 (s, 3H), 3.41 (d, *J* = 6.9 Hz, 2H), 3.32 (t, *J* = 2.4 Hz, 4H), 2.31 (s, 3H), 2.17 (s, 2H), 1.98 (s, 2H), 1.82 (s, 3H), 1.66 (s, 3H). ¹³C NMR (75 MHz, CDCl₃) δ 174.05, 172.92, 171.37, 163.60, 153.57, 144.18, 134.46, 122.92, 122.07, 116.84, 106.44, 70.09, 61.04, 40.31, 40.04, 35.22, 35.00, 23.18, 22.64, 16.13, 11.58. ESI-HRMS (*m/z*) calcd for C₂₁H₂₉N₂O₆⁺ [M+H]⁺: 405.20201, found: 405.20178.

4.1.15 (E)-6-(4-hydroxy-6-methoxy-7-methyl-3-oxo-1,3-dihydroisobenzofuran-5-yl)-4-methyl-N-(2-(piperidin-1-yl)ethyl)hex-4-enamide (E1)

White powder; yield 65%; m.p. 122-124°C. ¹H NMR (300 MHz, CDCl₃) δ 6.49 (s, 1H), 5.27 (t, *J* = 6.5 Hz, 1H), 5.18 (s, 2H), 3.78 (s, 3H), 3.46 – 3.29 (m, 4H), 2.71 – 2.41 (m, 6H), 2.32 (s, 4H), 2.15 (s, 3H), 1.83 (s, 3H), 1.64 (dt, *J* = 10.9, 5.6 Hz, 4H), 1.48 (d, *J* = 5.2 Hz, 2H). ¹³C NMR (75 MHz, CDCl₃) δ 173.01, 172.83, 163.45, 156.03, 144.27, 134.21, 123.96, 122.60, 114.97, 106.41, 69.64, 60.99, 57.20, 54.75(2C), 36.19, 35.24, 34.98, 25.45(2C), 23.94, 22.96, 15.97, 11.48. ESI-HRMS (*m/z*) calcd for C₂₄H₃₅N₂O₅⁺ [M+H]⁺: 431.25045, found: 431.25381.

4.1.16 **(E)-6-(4-hydroxy-6-methoxy-7-methyl-3-oxo-1,3-dihydroisobenzofuran-5-yl)-4-methyl-N-(2-(pyrrolidin-1-yl)ethyl)hex-4-enamide (E2)**

White powder; yield 59%; m.p. 130-132°C. ¹H NMR (300 MHz, CDCl₃) δ 6.69 (brs, 1H), 5.27 (t, *J* = 6.9 Hz, 1H), 5.18 (s, 2H), 3.80 (s, 3H), 3.41 (dd, *J* = 11.7 Hz, 5.4 Hz, 4H), 2.91 – 2.71 (m, 6H), 2.34 (s, 4H), 2.15 (s, 3H), 1.93-1.85 (m, 4H), 1.83 (s, 3H). ¹³C NMR (75 MHz, CDCl₃) δ 173.07(2C), 163.40, 156.58, 144.34, 134.18, 124.39, 122.74, 114.62, 106.47, 69.55, 60.99, 54.98, 54.48(2C), 37.76, 35.22, 34.88, 23.37(2C), 23.00, 15.99, 11.46. ESI-HRMS (*m/z*) calcd for C₂₃H₃₃N₂O₅⁺ [M+H]⁺: 417.23840, found: 417.23795.

4.1.17

(E)-N-(2-(1H-indol-3-yl)ethyl)-6-(4-hydroxy-6-methoxy-7-methyl-3-oxo-1,3-dihydroisobenzofuran-5-yl)-4-methylhex-4-enamide (E3)

White powder; yield 51%; m.p. 116-118°C. ¹H NMR (300 MHz, CDCl₃) δ 8.39 (s, 1H), 7.69 (s, 1H), 7.54 (d, *J* = 7.7 Hz, 1H), 7.37 (d, *J* = 8.0 Hz, 1H), 7.25 – 7.16 (m, 1H), 7.15 – 7.05 (m, 1H), 6.98 (d, *J* = 2.1 Hz, 1H), 5.67 (t, *J* = 5.4 Hz, 1H), 5.25 (t, *J* = 6.9 Hz, 1H), 5.00 (s, 2H), 3.77 (d, *J* = 6.3 Hz, 3H), 3.52 (dd, *J* = 12.9, 6.8 Hz, 2H), 3.38 (d, *J* = 6.9 Hz, 2H), 2.82 (t, *J* = 6.9 Hz, 2H), 2.36 – 2.20 (m, 4H), 2.09 (s, 3H), 1.80 (s, 3H). ¹³C NMR (75 MHz, CDCl₃) δ 173.00, 172.87, 163.59, 153.46, 144.21, 136.41, 134.51, 127.27, 122.83, 122.16, 122.00, 121.90, 119.19, 118.54, 116.83, 112.62, 111.36, 106.30, 70.04, 61.03, 39.78, 35.28, 35.04, 25.27, 22.62, 16.12, 11.50. ESI-HRMS (*m/z*) calcd for C₂₇H₃₁N₂O₅⁺ [M+H]⁺: 463.22275, found: 463.22253.

4.1.18 **(E)-6-(6-(4-benzylpiperazin-1-yl)-3-methyl-6-oxohex-2-en-1-yl)-7-hydroxy-5-methoxy-4-methylisobenzofuran-1(3H)-one (E4)**

White powder; yield 73%; m.p. 121-123°C. ¹H NMR (300 MHz, CDCl₃) δ 7.36 – 7.29 (m, 4H), 7.25 (dd, *J* = 8.8, 3.8 Hz, 1H), 5.27 – 5.22 (m, 1H), 5.20 (s, 2H), 3.77 (s, 3H), 3.59 (t, *J* = 4.8 Hz, 2H), 3.51 (s, 2H), 3.44 (t, *J* = 4.8 Hz, 2H), 3.39 (d, *J* = 6.8 Hz, 2H), 2.50 – 2.35 (m, 6H), 2.32-2.25 (m, 2H), 2.15 (s, 3H), 1.82 (s, 3H). ¹³C NMR (75 MHz, CDCl₃): δ 172.88, 171.18, 163.65, 153.57, 144.07, 137.47, 134.77, 129.15(2C), 128.31(2C), 127.28, 122.41, 122.19, 116.75, 106.36, 70.02, 62.82, 61.02, 53.11, 52.73, 45.54, 41.48, 35.02, 31.94, 22.63, 16.39, 11.57. ESI-HRMS (*m/z*) calcd for C₂₈H₃₅N₂O₅⁺ [M+H]⁺: 479.25405, found: 479.25369.

4.1.19 (E)-N-(3-(1H-imidazol-1-yl)propyl)-6-(4-hydroxy-6-methoxy-7-methyl-3-oxo-1,3-dihydroisobenzofuran-5-yl)-4-methylhex-4-enamide(E5)

White powder; yield 63%; m.p. 116-118°C. ¹H NMR (300 MHz, CDCl₃) δ 7.47 (s, 1H), 6.99 (d, *J* = 38.6 Hz, 2H), 5.69 (s, 1H), 5.28 (t, *J* = 11.6 Hz, 1H), 5.21 (s, 2H), 3.95 (t, *J* = 6.9 Hz, 2H), 3.77 (s, 3H), 3.44 (t, *J* = 16.4 Hz, 2H), 3.22 (dd, *J* = 12.8, 6.4 Hz, 2H), 2.30 (s, 4H), 2.15 (s, 3H), 2.02 – 1.89 (m, 2H), 1.83 (s, 3H). ¹³C NMR (75 MHz, CDCl₃) δ 173.15, 172.89, 163.61, 153.60, 144.17, 134.57(2C), 132.34, 122.90(2C), 122.12, 116.84, 106.44, 70.05, 61.04, 44.61, 36.58, 35.16, 34.91, 31.24, 22.67, 16.18, 11.57. ESI-HRMS (*m/z*) calcd for C₂₃H₃₀N₃O₅⁺ [M+H]⁺: 428.21800, found: 428.21771.

4.2 Materials needed for cell and animal experiments

3-(4,5-Dimethylthiazol-2-yl)-2,5-diphenyl-2*H*-tetrazolium bromide (MTT) was purchased from Sigma-Aldrich Co. (St. Louis, MO, USA). HFF-1 cell (Human Foreskin Fibroblasts-1) was purchased from American Type Culture Collection (ATCC, Manassas, VA, USA). *Toxoplasma gondii* is a highly virulent *Toxoplasma gondii* RH strain, which was donated by the Zoonoses Research Center, Won Kwang University School of Medicine, South Korea. The experimental animals were provided by the Animal Experiment Center of Yanbian University (license number SCXK 2011-0007), and are raised in the animal laboratory of the School of Pharmacy, Yanbian University, the experimental conditions meet the national laboratory animal requirements.

4.3 In vitro anti-*T. gondii* experiment

The cytotoxicity and anti-*T. gondii* activity of the compounds were tested by the classic MTT method. HFF-1 cells what in the logarithmic growth phase was collected, and inoculated in a 96-well plate (1×10⁴ cells per well), after 24 h of incubation, adding *Toxoplasma gondii* tachyzoites at a ratio of cells per well: *Toxoplasma gondii* = 1:5, continue to cultivate for 24 h, and then added different concentrations of test drugs (10-1000 μM), in addition, spiramycin and DMSO were used as a positive control and negative control respectively, the final concentration of DMSO solvent did not exceed 0.1%. After 24 h of incubation, 15 μL of MTT solution (0.5 mg/mL) was added to each well, the OD value (absorbance) was read on a microplate reader at a wavelength of 492 nm. The cytotoxicity of the tested drugs was determined under the same experimental conditions, except that the cells were not infected with *Toxoplasma gondii*, and the other operating methods were the same. After determining the OD value, the IC₅₀ of each group of cells and the selectivity index (SI) were calculated.

4.4 In vivo anti-*T. gondii* experiment

Thirty female KM mice were used for *in vivo* experiments. Six mice were randomly selected as the normal group without any treatment. The remaining 24 mice were used to establish an acute *Toxoplasma* infection animal model (*Toxoplasma gondii* was injected intraperitoneally in mice (2×10³/mouse)), which was then randomly divided into four groups (infected but not treatment group, Spiramycin group, MPA

group, E5 group), each group has six animals. Four hours after infection, each test compound was given to mice by gavage at 100 mg/kg once a day for four consecutive days. The untreated group was given the same dose of normal saline. On the 5th day, the mice's eye blood was collected and sacrificed by cervical dislocation. Their abdominal cavity was rinsed with sterile physiological saline to collect the parasites/tachyzoites. Those were counted under an optical microscope (BDS200 inverted microscope) to calculate the inhibitory rate of the drug on *Toxoplasma gondii*. At the same time, the liver and spleen were dissected, and the liver and spleen index, serum alanine aminotransferase (ALT), aspartate aminotransferase AST, liver homogenate glutathione GSH, and malondialdehyde MDA were determined. Moreover record the weight change of mice during the administration period.

4.4.1 The liver and spleen index assay

After the mice of each group were sacrificed by neck dissection, they were dissected, the liver and kidney of the mice were separated, and the weight of the liver and spleen of each mouse was weighed and recorded, and then the liver and spleen index was obtained. The dissected liver and spleen were stored at low temperature, and the unused internal organs were temporarily stored in a refrigerator at -80 °C.

Liver (spleen) index (%) = [wet weight of liver/spleen (g) / body weight of mice (g)] × 100%

4.4.2 Determination of ALT and AST in serum

The determination of AST and ALT in serum is based on Lai's method. An appropriate amount of serum was mixed with 5 times the amount of ALT or AST matrix buffer, then it was placed at 37°C for 30 min, and 1 mmol/L 2,4-dinitrophenylhydrazine solution equal in volume was added to the matrix buffer and mixed well, after 20 min, 0.4 mol/L sodium hydroxide solution was added and placed at room temperature for 5 min. Adjusting the zero with distilled water at a wavelength of 505 nm, the absorbance of each sample was read and calculated, and obtained the concentration of ALT and AST in the serum (U/L) through the standard curve^[52].

ALT matrix buffer: 1.79 g of DL-alanine and 29.2 mg of α-ketoglutarate were accurately weighed, and dissolved using an appropriate amount of 0.1 mol/L phosphate buffer. After that, 1 mol/L of sodium hydroxide solution was added to adjust the pH to 7.4. Finally, additional phosphate buffer was added to adjust the volume to 100 ml to obtain the ALT matrix buffer (stored at 4°C).

AST matrix buffer: 24.2 mg α-ketoglutarate and 2.66g DL-aspartic acid were accurately weighed, and dissolved using appropriate amount of 0.1 mo/L phosphate buffer. After that, 1 mol/L of sodium hydroxide solution was added to adjust the pH to 7.4. Finally, Finally, additional phosphate buffer was added to adjust the volume to 100 ml to obtain the AST matrix buffer (stored at 4°C).

4.4.3 Determination of GSH and MDA in liver homogenate

Preparation of liver homogenate: A certain amount of liver tissue was washed using pre-cooled physiological saline, and then an electric homogeniser was used to prepare a 20% tissue homogenate in

0.85% normal saline after drying. Followed by centrifugation (4000 rpm, 10 min), the supernatant was taken as a liquid reserve. The whole process should be carried out at low temperature as much as possible.

Protein content determination: The protein content of each group of mouse liver homogenate was tested according to the BCA protein concentration determination kit (Shanghai Biyuntian Biotechnology Co., Ltd.).

GSH determination: An appropriate amount of liver homogenate supernatant was mixed according to the supernatant: 20% trichloroacetic acid = 2:1, followed by centrifugation (4000 rpm, 10 min). Subsequently, the prepared 0.3 mol/L disodium hydrogen phosphate buffer and 0.04% DTNB reagent were added in sequence and mixed thoroughly, and then the absorbance value was measured at 412 nm. In the experiment, the GSH standard curve was drawn with glutathione standard substance and the regression equation was obtained. Substituting the measured absorbance value of the experimental sample into the regression equation, the concentration of GSH in each sample solution can be calculated. Finally, the GSH content in the liver homogenate (mg/gprot) = the measured GSH concentration in the sample solution (mg/ml) / the liver homogenate protein concentration (gprot/ml)^[53].

MDA determination: MDA is determined by the thiobarbituric acid method. A certain amount of liver homogenate supernatant was mixed with 0.5% thiobarbituric acid, and then it was boiled in a water bath for 1 h, centrifuged after cooling (6000 rpm, 10 min). Moreover the upper pink clear liquid was measured absorbance value at 532 nm. In addition, 1,1,2,2-tetraethoxypropane was used as a standard sample to draw a standard curve, and the absorbance value of the experimental sample was substituted into the standard curve to obtain the MDA concentration of each sample solution. Finally, the MDA content in the liver homogenate (μmol/gprot) = the measured MDA concentration in the sample solution (μmol/ml) / the liver homogenate protein concentration (gprot/ml)^[54].

Declarations

Acknowledgements

This work was supported by the National Natural Science Foundation of China (No.81960626) and the Higher Education Discipline Innovation Project (111 Project, D18012). Thanks for the language editing service provided by the Cactus Communications (Shanghai) Co., Ltd. for the manuscript.

Declaration of competing interest

The authors declare no conflict of interest.

References

1. Luder CG, Bohne W, Soldati D (2001) Toxoplasmosis: a persisting challenge. *Trends Parasitol* 17:460–463
2. Osunkalu VO, Akanmu SA, Ofomah NJ et al (2011) Seroprevalence of *Toxoplasma gondii* IgG antibody in HIV-infected patients at the Lagos University teaching hospital. *HIV AIDS (Auckl)* 3:101–105
3. Lang C, Grob U, Luder CGK (2007) Subversion of innate and adaptive immuneresponses by *Toxoplasma gondii*. *Parasitol Res* 100:191–203
4. Innes EA (2010) A brief history and overview of *Toxoplasma gondii*. *Zoonoses Public Hlth* 57:1–7
5. Bianchi G. Lipids and phenols in table olives. *Eur J Lipid Sci Technol* 2003;105: 229 – 242
6. Schoondermark-van de Ven E, Vree T, Melchers W et al (1995) In vitro effects of sulfadiazine and its metabolites alone and in combination with pyrimethamine on *Toxoplasma gondii*. *Antimicrob Agents Ch* 39:763–765
7. Borkowski PK, Brydak-Godowska J, Basiak W et al (2018) Adverse reactions in antifolate-treated toxoplasmic retinochoroiditis. *Curr Trends Immunity Respiratory Infect* 1108:37–48
8. Adeyemi OS, Murata Y, Sugi T et al (2017) Inorganic nanoparticles kill *Toxoplasma gondii* via changes in redox status and mitochondrial membrane potential. *Int J Nanomed* 12:1647–1661
9. Ramos-Casals M, Font J (2005) Mycophenolate mofetil in patients with hepatitis C virus infection. *Lupus* 14:64–72
10. Chan TM, Li FK, Tang CS (2000) Efficacy of mycophenolate mofetil in patients with diffuse proliferative lupus nephritis. *N Engl J Med* 343:1156–1162
11. Schlitt HJ, Barkmann A, Boker KH (2001) Replacement of calcineurin inhibitors with mycophenolate mofetil in liver-transplant patients with renal dysfunction: a randomised controlled study. *Lancet* 357:587–591
12. Siebert A, Wysocka M, Krawczyk B et al (2018) Synthesis and antimicrobial activity of amino acid and peptide derivatives of mycophenolic acid. *Eur J Med Chem* 143:646–655
13. Yin YB, Wang YJ, Dang W et al (2016) Mycophenolic acid potently inhibits rotavirus infection with a high barrier to resistance development. *Antivir Res* 133:41–49
14. Tsolaki E, Eleftheriou P, Kartsev V et al (2018) Application of Docking Analysis in the Prediction and Biological Evaluation of the Lipoygenase Inhibitory Action of Thiazolyl Derivatives of Mycophenolic Acid. *Molecules* 23:1621
15. Prejs M, Cholewinski G, Siebert A et al (2016) New conjugates of mycophenolic acid and their antiproliferative activity. *J Asian Nat Prod Res* 18:1057–1062
16. Castro-Elizalde KN, Hernández-Contreras P, Ramírez-Flores CJ (2018) Mycophenolic acid induces differentiation of *Toxoplasma gondii* RH strain tachyzoites into bradyzoites and formation of cyst-like structure in vitro. *Parasitol Res* 117:563
17. Halle MB, Lee W, Yudhistira T et al. Mycophenolic Acid: Biogenesis, Compound Isolation, Biological Activity, and Historical Advances in Total Synthesis. *Eur J Org Chem* 2019;2315–2334

18. Guo HY, Jin CM, Zhang HM et al (2019) Synthesis and Biological Evaluation of (+)-Usnic Acid Derivatives as Potential Anti-Toxoplasma gondii Agents. *J Agric Food Chem* 67:9630–9642
19. Zhang HJ, Zhang GR, Piao HR et al (2017) Synthesis and characterisation of celastrol derivatives as potential anticancer agents. *J Enzym Inhib Med Chem* 33:190–198
20. Zhang TY, Li C, Li YR et al (2016) Synthesis and Antimicrobial Evaluation of Aminoguanidine and 3-amino-1,2,4-triazole Derivatives as Potential Antibacterial Agents. *Lett Drug Des Dis* 13(10):1063–1075
21. Figueiredo SAC, Salvador JAR, Cortés R, Cascante M (2017) Design, synthesis and biological evaluation of novel C-29 carbamate celastrol derivatives as potent and selective cytotoxic compounds. *Eur J Med Chem* 139:836–848
22. Voynikov Y, Valcheva V, Momekov G (2014) Theophylline-7acetic acid derivatives with amino acids as anti-tuberculosis agents. *Bioorg Med Chem Lett* 24:3043–3045
23. Pang L, Liu CY, Gong GH et al (2020) Synthesis, in vitro and in vivo biological evaluation of novel lappaconitine derivatives as potential anti-inflammatory agents. *Acta Pharmaceutica Sinica B* 10:628–645
24. Bian M, Zhen D, Shen QK et al (2021) Structurally modified glycyrrhetic acid derivatives as anti-inflammatory agents. *Bioorg Chem* 107:104598
25. Zhang HB, Shen QK, Wang H et al (2018) Synthesis and evaluation of novel arctigenin derivatives as potential anti-Toxoplasma gondii agents. *Eur J Med Chem* 158:414–427
26. Luan T, Jin CM, Jin C-M et al (2019) Synthesis and biological evaluation of ursolic acid derivatives bearing triazole moieties as potential anti-Toxoplasma gondii agents. *J Enzym Inhib Med Ch* 34:761–772
27. Drag ZM, Kulbacka J, Saczko J et al (2009) Esters of betulin and betulinic acid with amino acids have improved water solubility and are selectively cytotoxic toward cancer cells. *Bioorg Med Chem Lett* 19:4814–4817
28. Lin JC, Cherng JM, Hung MS et al (2008) Inhibitory effects of some derivatives of glycyrrhizic acid against Epstein-Barrvirus infection: structure-activity relationships. *Antivir Res* 79:6–11
29. Schwarz S, Csuk R (2010) Synthesis and antitumour activity of glycyrrhetic acid derivatives. *Bioorg Med Chem Lett* 18:7458–7474
30. Kortagere S, Mui E, McLeod R et al (2011) Rapid discovery of inhibitors of Toxoplasma gondii using hybrid structure-based computational approach. *J Comput Aided Mol Des* 25:403–411
31. Kadri D, Crater AK, Lee H et al (2014) The potential of quinoline derivatives for the treatment of toxoplasma gondii infection. *Exp Parasitol* 145:135–144
32. Fang YQ, Zhang HJ, Ren Y et al (2018) Synthesis and Evaluation of the Antidepressant Activity of Quinoxaline-2,3(1H,4H)-dione Derivatives. *Lat Am J Pharm* 37(1):170–181
33. Davies JR, Kane PD, Moody CJ et al (2005) Control of competing N-H insertion and Wolff rearrangement in dirhodium(II)-Catalyzed reactions of 3-indolyl diazoketoesters. *Synthesis of a*

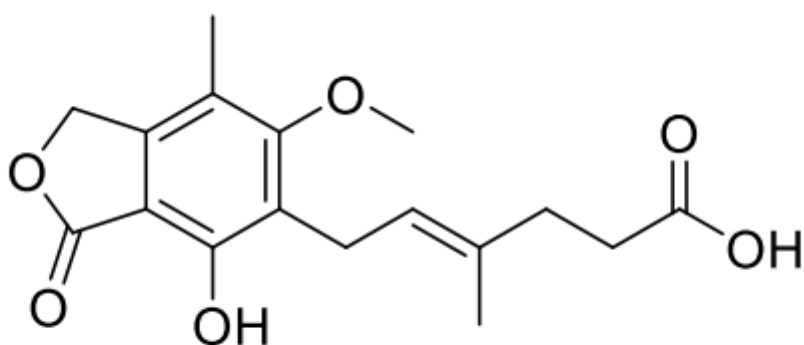
- potential precursor to the marine 5-(3-indolyl)oxazole martefragin A. *J Org Chem* 70:5840–5851
34. Beckmann HSG, Nie F, Hagerman CE et al (2013) A strategy for the diversity-oriented synthesis of macrocyclic scaffolds using multidimensional coupling. *Nat Chem* 5:861–867
 35. Agnieszka S, Magdalena W, Beata K et al (2018) Synthesis and antimicrobial activity of amino acid and peptide derivatives of mycophenolic acid. *Eur J Med Chem* 143:646–655
 36. Chetan PS, Prashant SK (2018) Newer human inosine 5'-monophosphate dehydrogenase 2 (hIMPDH2) inhibitors as potential anticancer agents. *J Enzym Inhib Med Ch* 33:972–977
 37. Deng H, Huang X, Jin CM et al (2020) Synthesis, in vitro and in vivo biological evaluation of dihydroartemisinin derivatives with potential anti-Toxoplasma gondii agents. *Bioorg Chem* 94:103467
 38. Dubey JP (2009) History of the discovery of the life cycle of Toxoplasma gondii. *Int J Parasitol* 39:877–882
 39. Mordue DG, Monroy F, Regina M et al (2001) Acute toxoplasmosis leads to lethal overproduction of the cytokines. *J Immunol* 167:4574
 40. Ustun S, Aksoy U, Dagci H, Galip E (2004) Frequency of toxoplasmosis in patients with cirrhosis. *World J Gastroenterol* 10:452–454
 41. Mordue DG, Monroy F, Regina ML, Dinarello CA, Sibley D (2001) Acute toxoplasmosis leadsto lethal overproduction of Th1 cytokines. *J Immunol* 167:4574–4584
 42. Znalesniak E, Fu T, Salm F et al (2017) Transcriptional responses in the murine spleen after toxoplasma gondii infection: inflammasome and mucus-associated genes. *Int J Mol Sci* 18:1245
 43. Cho CW, Han CJ, Rhee YK (2015) Cheonggukjang polysaccharides enhance immune activities and prevent cyclophosphamide-induced immunosuppression. *In J Biol Macromol* 72:519–525
 44. Autier B, Dion S, Robert-Gangneux F (2018) The liver as an organ at risk for Toxoplasma transmission during transplantation: myth or reality? *J Clin Pathol* 71:763–766
 45. Choi HJ, Yu ST, Lee KI et al (2014) 6-Trifluoromethyl-2-thiouracil possesses anti-Toxoplasma gondii effect in vitro and in vivo with low hepatotoxicity. *Exp Parasitol* 143:24–29
 46. Elsheikha HM, El-Motayam MH, Abouel-Nour MF, Morsy AT (2009) Oxidative stress and immune-suppression in Toxoplasma gondii positive blood donors: implications for safe blood transfusion. *J Egypt Soc Parasitol* 39:421–428
 47. Smith GR, Shanley GR (2013) Computational modelling of the regulation of Insulin signaling by oxidative stress. *BMC Syst Boil* 7:41–60
 48. Kikuchiueda T, Ubagai T, Ono Y (2013) Priming effects of tumor necrosis -a on production of reactive oxygen species during Toxoplasma gondii stimulation and receptor gene expression in differentiated HL-60 cells. *J Infect Chemother* 19:1053–1064
 49. Yang J, Dong S, Zhu H, Jiang Q, Yang J (2013) Molecular and expression analysis of manganese superoxide dismutase (Mn-SOD) gene under temperature and starvation stress in rotifer Brachionus calyciflorus. *Mol Biol Rep* 40:2927–2937

50. Ebisch IMW, Thomas CMG, Peters WHM, Braat DDM, SteegersTheunissen RPM (2007) The importance of folate, zinc and antioxidants in the pathogenesis and prevention of subfertility. *Hum Reprod Update* 13:163–174
51. Grotto D, Maria LS, Valentini J, Paniz C, Schitt G, Garcia SC (2009) Importance of the lipidperoxidation biomarkers and methodological aspects for malondialdehyde quantification. *Quim Nova* 32:169–174
52. Jiang JH, Jin CM, Kim YC et al (2008) Anti-toxoplasmosis effects of oleuropein isolated from *fraxinus rhychophylla*. *Biol Pharm Bull* 31:2273–2276
53. Reitman S, Frankel S (1957) A colorimetric method for the determination of serum glutamic oxalacetic and glutamic pyruvic transaminases. *Am J Clin Pathol* 28:56–63
54. Griffith OW (1980) Determination of glutathione and glutathione disulfide using glutathione reductase and 2-vinylpyridine. *Anal Biochem* 106:207–212

Tables

Due to technical limitations, table 1-2 is only available as a download in the Supplemental Files section.

Figures



mycophenolic acid

Figure 1

The structure of mycophenolic acid.

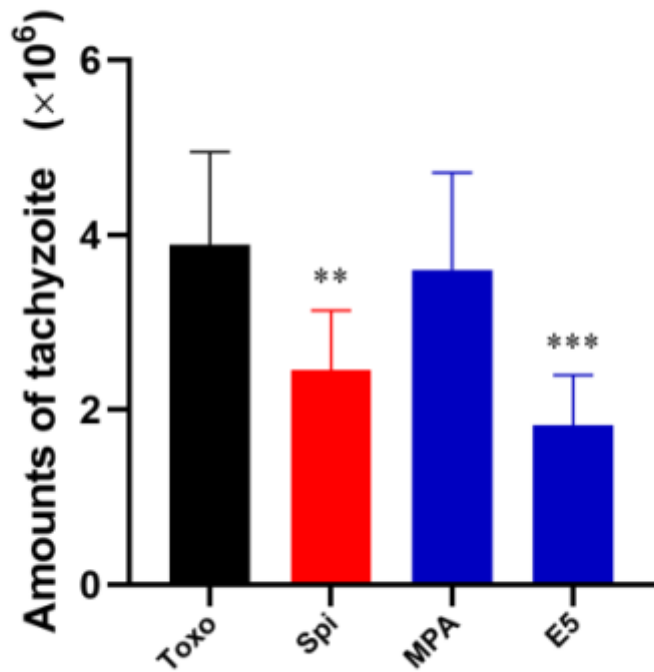


Figure 2

Number (Mean \pm SD) of tachyzoites in the peritoneal cavity of mice treated with the test compounds, n = 6; ** P < 0.01 and *** P < 0.001 compared with Toxo; # P < 0.05 compared with Spi.

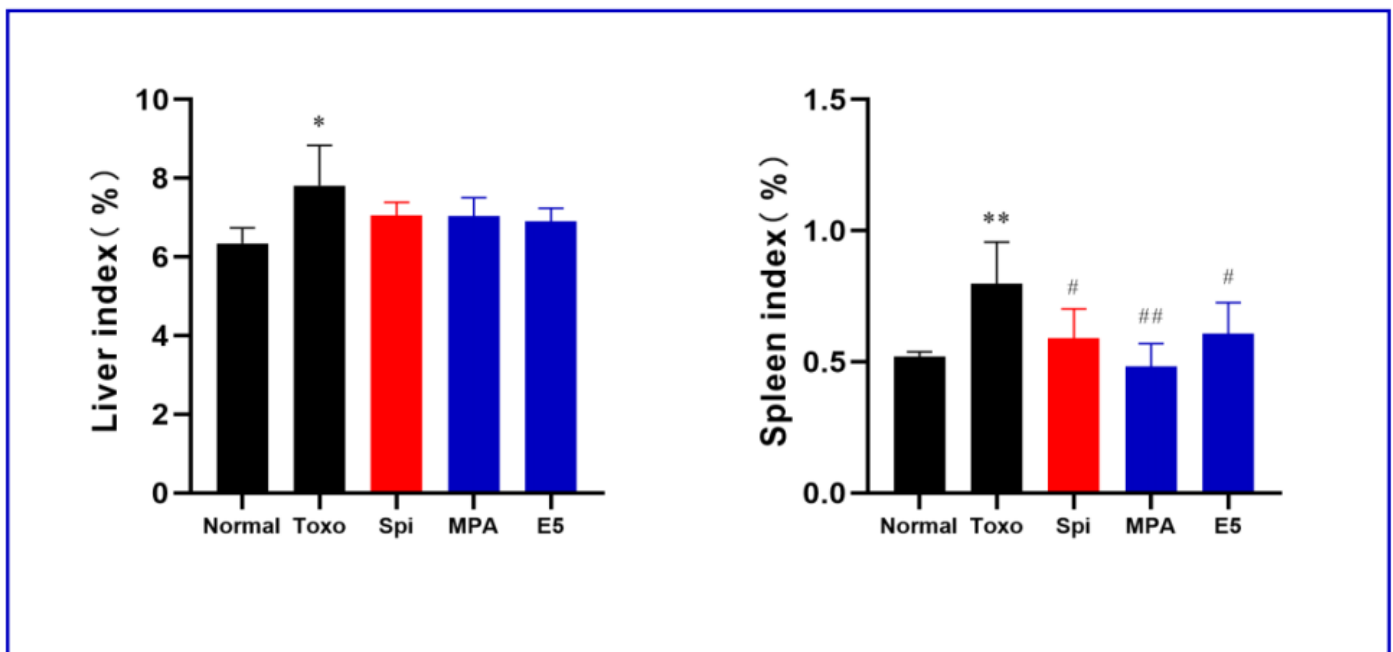


Figure 3

Effects of the test compounds on relative organ weights in *Toxoplasma gondii*-infected KM mice. Values are expressed as mean \pm S.D. (n = 6). *P < 0.05 and **P < 0.01 compared with normal; # P < 0.05 and ## P < 0.01 compared with Toxo.

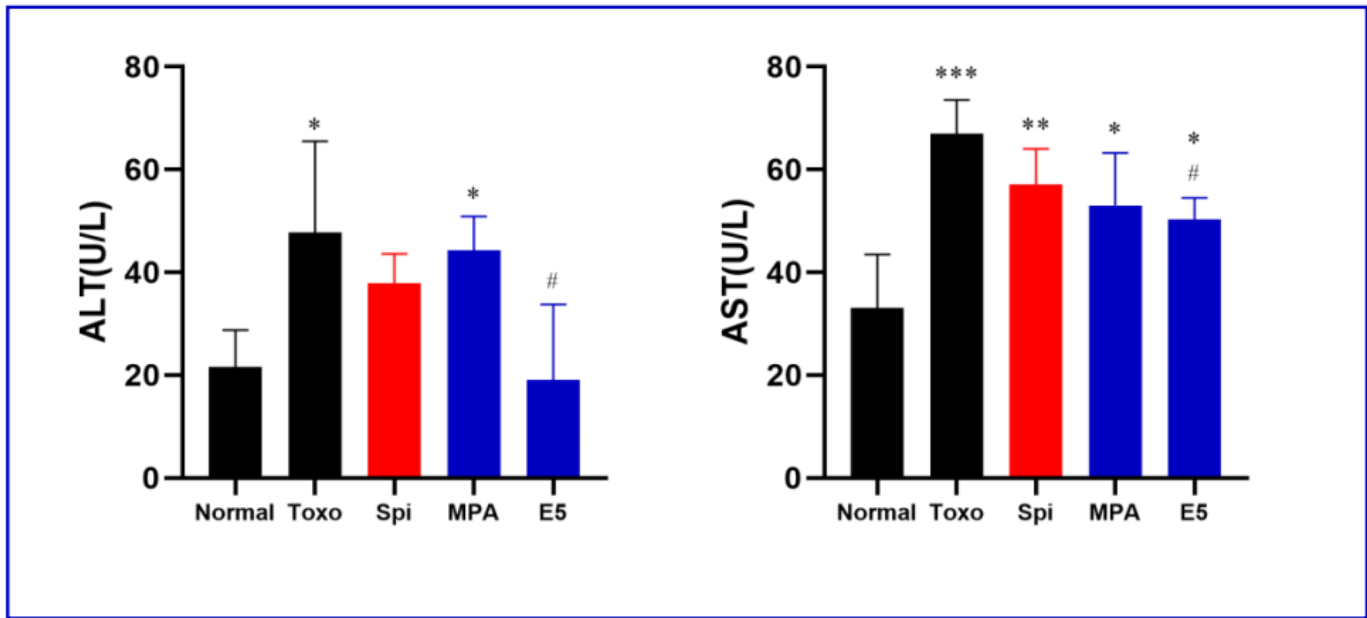


Figure 4

Effects of the text compounds on ALT and AST levels in *Toxoplasma gondii*-infected KM mice. Values are expressed as mean \pm S.D. (n = 6). *P < 0.05, **P < 0.01 and ***P < 0.001 compared with normal; # P < 0.05 compared with Toxo.

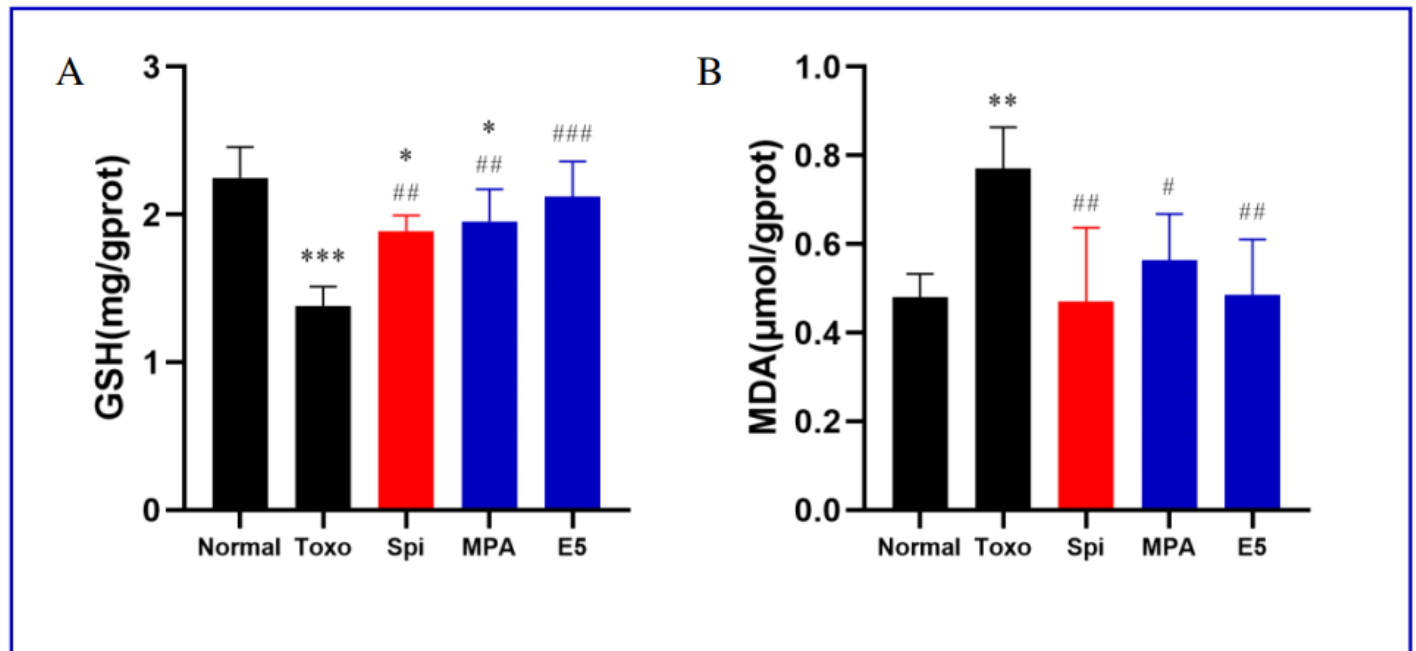


Figure 5

Effect of the test compounds on GSH and MDA levels in *Toxoplasma gondii*-infected KM mice. Values are expressed as mean \pm S.D. (n = 6). *P < 0.05, **P < 0.01 and ***P < 0.001 compared with normal; # P < 0.05, ## P < 0.01 and ### P < 0.001 compared with Toxo.

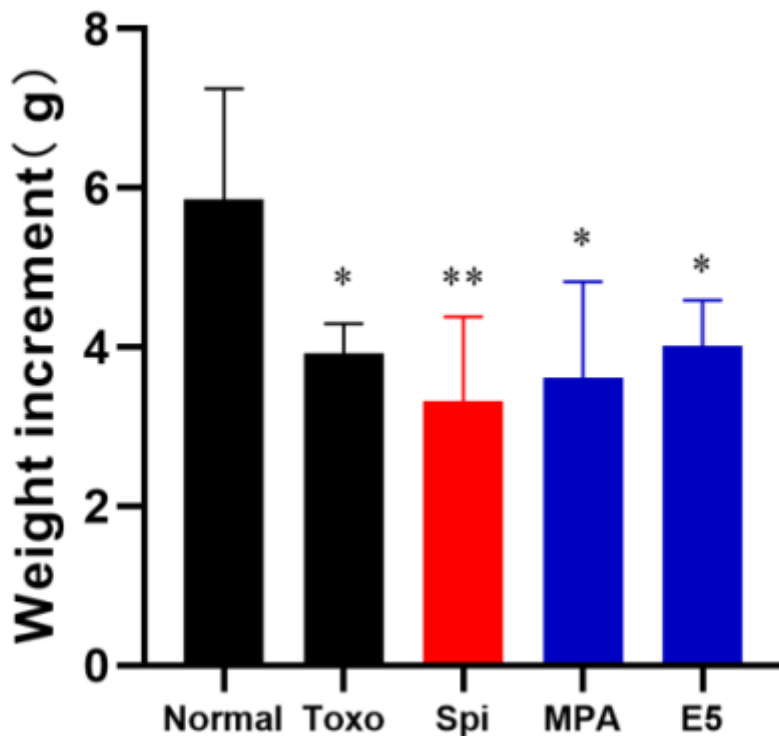


Figure 6

Effect of the test compounds on the body weights of *Toxoplasma gondii*-infected KM mice. Values are expressed as mean \pm S.D. (n = 6). *P < 0.05, **P < 0.01 and ***P < 0.001 compared with normal; #P < 0.05 compared with Toxo.

Supplementary Files

This is a list of supplementary files associated with this preprint. Click to download.

- [Supplementarymaterials.docx](#)
- [Tables.pdf](#)
- [Scheme1.png](#)